Formation of fragments in heavy-ion collisions using a modified clusterization method

Supriya Goyal and Rajeev K. Puri*
Department of Physics, Panjab University, Chandigarh-160 014, India
(Received 5 June 2010; revised manuscript received 9 November 2010; published 7 April 2011)

We study the formation and stability of the fragments by extending the minimum spanning tree method (MST) for clusterization. In this extension, each fragment is subjected to a binding-energy check calculated using the modified Bethe-Weizsäcker formula. Earlier, a constant binding-energy cut of 4 MeV/nucleon was imposed. Our results for ^{197}Au + ^{197}Au collisions are compared with ALADiN data and also with the calculations based on the simulated annealing technique. We shall show that the present modified version improves the agreement compared to the MST method.

DOI: 10.1103/PhysRevC.83.047601 PACS number(s): 25.70.Pq, 21.30.Fe, 24.10.Lx

Multifragmentation has been of central interest in the last two decades. The primary cause of this intense investigation is the rich information associated with the production and emission of fragments [1,2]. A large number of sophisticated experiments have been performed during the last two decades to detect the fragments and to look for their associated properties [2,3]. An equal number of attempts are also reported in the literature on the theoretical front [1,4–6].

On the theoretical front, dynamical approaches such as quantum molecular dynamics (QMD) [1] and Boltzmann-Uehling-Uhlenbeck (BUU) [7] follow the time evolution of the reactions from the initial to the final stage. One, however, needs secondary algorithms to identify the fragments. One has always struggled for a proper algorithm for identifying these fragments. Early attempts consist of identifying the fragments based on their spatial correlations. This approach is often dubbed as the minimum spanning tree (MST) algorithm [1,4,5]. This approach has been quite successful in explaining the fragmentation, especially at low incident energies [8]. One of the major problems with the MST method is that it does not guarantee the production of proper bound fragments. As a result, more sophisticated algorithms such as the early cluster recognition algorithm (ECRA) [9] and the simulated annealing clusterization algorithm (SACA) [6] were developed. These methods, although promising, are very complicated and can not be used as freely as the MST method. In addition, procedural steps such as cooling parameters, iterative procedure, and the choice of the minima can lead to an entirely different configuration of the fragments [6]. In mildly excited or in asymmetric reactions, the minimum is not sharp, therefore, the utility and scope of these algorithms is limited. To avoid the creation of spurious fragments, the MST method was improved by constraining the fragments to an average binding energy of 4 MeV/nucleon. Here, we further improve this method by subjecting each fragment to its corresponding binding energy. This will further enhance the predictive power of the MST method by discarding spurious fragments. For this paper, we generate the phase space using the quantum molecular dynamics model [1].

In our calculations, reactions are followed until saturation time which, in this study, is between 200 and 300 fm/c and fragments are then identified. In the MST method, two nucleons share the same fragment if their spatial distance is less than or equal to 4 fm, i.e., $|\mathbf{r}_\alpha - \mathbf{r}_\beta| \leqslant 4$ fm. In earlier work [5], one of us and co-workers imposed a binding-energy cut of 4 MeV/nucleon for all fragments with mass $A \geqslant 3$. Any cluster that failed to fulfill the condition was treated as a group of free nucleons. This version was labeled as MSTB(1.1). The condition of 4 MeV/nucleon is a rather crude approximation, and fragments may not be realistic. In this paper, we extend this method by imposing a microscopic binding-energy check.

One of the earlier attempts to reproduce the gross features of nuclear binding energies was made by Weizsäcker *et al.* [10]. The Bethe-Weizsäcker (BW) mass formula for the binding energy of a nucleus reads as [11]

$$E_{\rm bind}^{\rm BW} = a_v N_f - a_s N_f^{2/3} - a_c \frac{N_f^z\left(N_f^z-1\right)}{N_f^{1/3}} - a_{\rm sym}\frac{\left(N_f-2N_f^z\right)^2}{N_f} + \delta. \quad (1)$$

Here, N_f and N_f^z stand for the fragment size and proton number of a fragment. The various terms involved in this mass formula are the volume, surface, Coulomb, asymmetry, and pairing terms. The strength of different parameters is a_v = 15.79 MeV, a_s = 18.34 MeV, a_c = 0.71 MeV, and $a_{\rm sym}$ = 23.21 MeV, respectively [11]. δ corresponds to the pairing term.

This formula reproduces the binding energy of stable nuclei but faces a serious problem for light nuclei along the drip line and for nuclei with rich neutron or proton content. The inadequacy of BW mass formula for lighter nuclei was removed by Samanta *et al.* [11] by modifying its asymmetry and pairing terms. This modified formula was dubbed as the modified Bethe-Weizsäcker mass (BWM) formula [11]. In the BWM formula, the binding energy of a fragment is defined as [11]

$$E_{\rm bind}^{\rm BWM} = a_v N_f - a_s N_f^{2/3} - a_c \frac{N_f^z\left(N_f^z-1\right)}{N_f^{1/3}} - a_{\rm sym}\frac{\left(N_f-2N_f^z\right)^2}{N_f\left(1+e^{-N_f/17}\right)} + \delta_{\rm new}. \quad (2)$$

*rkpuri@pu.ac.in

The strength of various parameters now reads as $a_v = 15.777$ MeV, $a_s = 18.34$ MeV, $a_c = 0.71$ MeV, and $a_{\rm sym} = 23.21$ MeV, respectively. The pairing term $\delta_{\rm new}$ is given by

$$\delta_{\rm new} = +a_p N_f^{-1/2}(1 - e^{-N_f/30}) \text{ for even } N_f^z - \text{even } N_f^n, \quad (3)$$

$$\delta_{\rm new} = -a_p N_f^{-1/2}(1 - e^{-N_f/30}) \text{ for odd } N_f^z - \text{odd } N_f^n, \quad (4)$$

$$\delta_{\rm new} = 0 \text{ for odd } N_f \text{ nuclei}, \quad (5)$$

with $a_p = 12$ MeV. We extend the MSTB(1.1) method by subjecting each cluster to the above binding-energy criteria. This version of implementation is labeled as MSTB(2.1). Note that, in contrast to the restructured aggregation model (RAM), we do not reshape the fragments [12]. Since fragments at the final stage (i.e., after 200–300 fm/c) are cold, the above binding-energy criteria are justified [6]. Summarizing, if a MST cluster does not fulfill the stability criterium, a new cluster is built by taking off a single nucleon, which is then considered as a free particle. This procedure is repeated for each nucleon of the original MST cluster, and the most bound configuration is chosen. If all considered configurations contain clusters with a total energy higher than the one given by the mass formula, all nucleons of the MST cluster are considered as free.

We also note that, using the lattice gas model (LGM), the energy-based cluster recognization algorithm has also been applied for nuclear fragmentation [13].

For this analysis, we use a soft equation of state along with an energy-dependent nucleon-nucleon cross section. For details, the reader is referred to Ref. [1]. We shall here concentrate on the ^{197}Au + ^{197}Au reaction from low to relativistic energies.

In Fig. 1, we display the time evolution of the heaviest fragment ($A^{\rm max}$), free nucleons, light charged particles (LCPs) $2 \leqslant A \leqslant 4$, medium mass fragments (MMFs) $3 \leqslant A \leqslant 14$, intermediate mass fragments (IMFs) $5 \leqslant A \leqslant 65$ as well as fragments with masses $5 \leqslant A \leqslant 9$, $6 \leqslant A \leqslant 8$, and $9 \leqslant A \leqslant 12$ detected in the MST, MSTB(1.1), and MSTB(2.1) versions. For comparison, we also display the results with the simulated annealing clusterization algorithm [SACA(2.1)] that searches for the most bound configuration [6]. It is worth mentioning

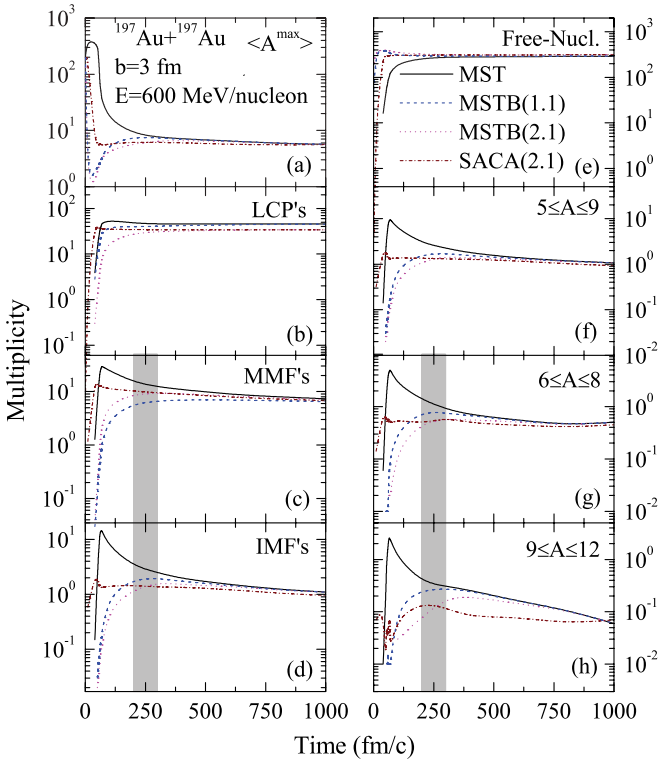

FIG. 1. (Color online) The time evolution of different fragments in the central reaction of ^{197}Au + ^{197}Au at 600 MeV/nucleon. Here we display (a) the heaviest fragment ($A^{\rm max}$) and (e) multiplicity of free nucleons, (b) light charged particles (LCPs) $2 \leqslant A \leqslant 4$, (c) medium mass fragments (MMFs) $3 \leqslant A \leqslant 14$, (d) intermediate mass fragments (IMFs) $5 \leqslant A \leqslant 65$, as well as (f) fragments with masses $5 \leqslant A \leqslant 9$, (g) $6 \leqslant A \leqslant 8$, and (h) $9 \leqslant A \leqslant 12$. The results obtained with the MST, MSTB(1.1), and MSTB(2.1) methods are shown, respectively, by solid, dashed, and dotted lines. We also display the results with SACA(2.1) (dashed-dotted line). The shaded area is for the time zone between 200–300 fm/c.

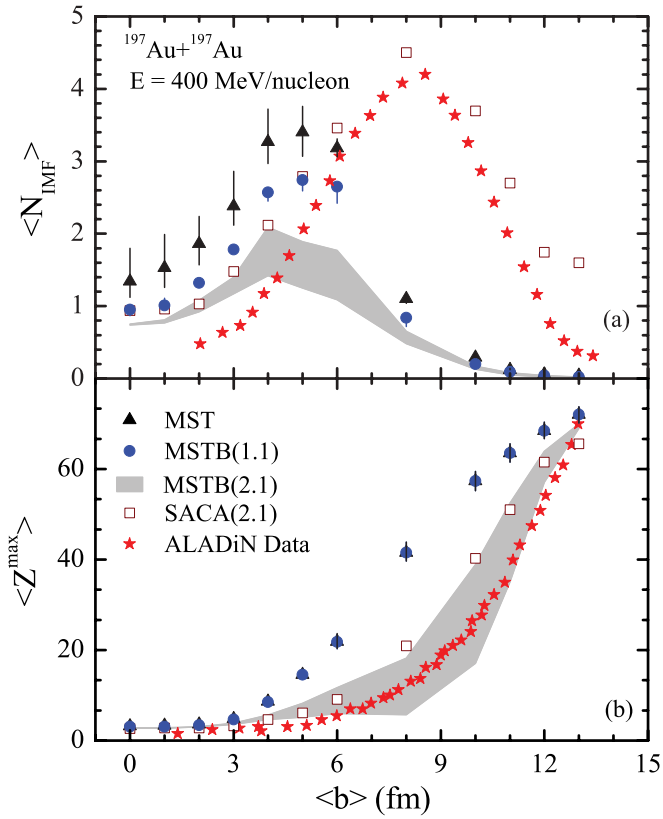

FIG. 2. (Color online) The multiplicity of (a) IMF's and (b) charge of heaviest fragment as a function of impact parameter for the reaction of ^{197}Au + ^{197}Au at 400 MeV/nucleon. The mean values in the MST and MSTB(1.1) methods at 250 fm/c are represented by symbols, whereas error bars in the MST and MSTB(1.1) methods denote the values at times between 200–300 fm/c. The corresponding values in the MSTB(2.1) method are denoted by gray shade. The results of SACA(2.1) are also shown by open squares. The experimental data points have been extracted from Ref. [2].

that in the SACA(2.1) algorithm, physical configuration is supposed to occur at a time of minima in the A^{max}, which is often around 60 fm/c. This minima, however, is not always sharp. Therefore, results can vary in many cases. Since the MST method does not consider the binding-energy check, A^{max} detected at high density shows 394 nucleons that decay afterwards. In fact, this is not properly bound as is evident from the MSTB(2.1) method. Even a constant binding-energy check of 4 MeV/nucleon does not yield proper results. The present modified version MSTB(2.1) yields results closer to the SACA(2.1) method and are, therefore, close to the reality. We noted from Fig. 1 that A^{max} and multiplicities of LCPs, MMFs, and IMFs are reduced from 8.6, 46.7, 14.0, and 3.2 formed in the MST method to 5.8, 30.0, 9.2, and 1.3, respectively, at 250 fm/c, once the realistic microbinding-energy check is employed. We notice reasonable differences with different versions of the MST method at 200–300 fm/c.

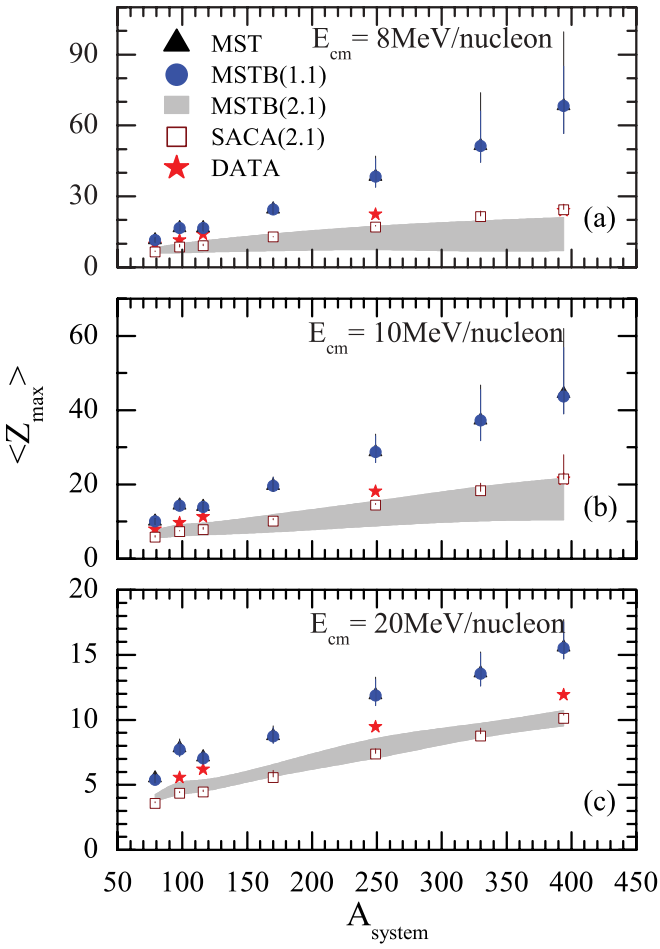

FIG. 3. (Color online) The heaviest bound charge as a function of the system mass for central collisions and at center-of-mass energy of (a) 8, (b) 10, and (c) 20 MeV/nucleon. The mean values in the MST and MSTB(1.1) methods at 250 fm/c are represented by symbols, whereas error bars in the MST and MSTB(1.1) methods denote the values at time between 200–300 fm/c. The corresponding values in the MSTB(2.1) method are denoted by gray shade. The results of SACA(2.1) are also shown by open squares. The experimental data points have been extracted from Ref. [14].

We display in Fig. 2 the multiplicity of intermediate mass fragments and mean charge of the heaviest fragment (Z^{max}) as a function of impact parameter for the fragments detected in the forward hemisphere as per ALADiN setup. The error bars in the theoretical results indicate variation in the multiplicity [in the MST and MSTB(1.1) methods] between 200–300 fm/c. The corresponding values in the MSTB(2.1) method are shown by the shaded portion. We also display the results of the ALADiN experimental setup [2] and SACA(2.1) for comparison. We see that the proper binding-energy check [i.e., MSTB(2.1) method] improves the agreement with ALADiN experimental data compared to MST and MSTB(1.1) methods. Although the multiplicity of IMFs is not reproduced by the new implementation, the $\langle Z_{max} \rangle$ is very well reproduced by MSTB(2.1). Similar results were also obtained at 600 MeV/nucleon. The underestimation of IMFs is not surprising since it is well known that even the MST method does not reproduce the trend. The MSTB(2.1) method will not create additional fragments; rather, it refines the fragments.

In Fig. 3, we display the comparison of heaviest bound charge Z_{max} obtained at center-of-mass energy of 8, 10, and 20 MeV/nucleon for the reactions of Ar + KCl, Ar + Ni, Ni + Ni, Rb + Rb, Xe + Sn, Ho + Ho, and Au + Au using MST, MSTB(1.1), MSTB(2.1), and SACA(2.1) methods. Again, we see that this implementation yields results close to the experimental data even at the lower tail of incident energies, where fragmentation is a rare phenomena [14].

In Fig. 4, we display the charge yields of fragments obtained in the reaction of ^{197}Au + ^{197}Au at incident energy of 150 and 250 MeV/nucleon average over central and semicentral collisions. Very interestingly, we see that the MSTB(2.1) gives results as good as SACA(2.1) and, thus, is able to explain the data nicely [15].

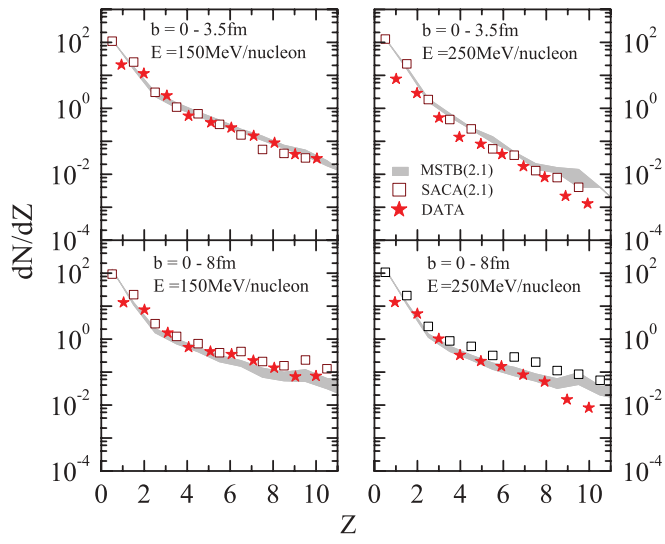

FIG. 4. (Color online) The charge distribution for ^{197}Au + ^{197}Au at (a), (b) 150 and (c), (d) 250 MeV/nucleon average over (a), (c) central and (b), (d) semicentral collisions. The mean values in the MSTB(2.1) method at 200–300 fm/c are denoted by gray shade. The results of SACA(2.1) are also shown by open squares. The experimental data points are extracted from Ref. [15].

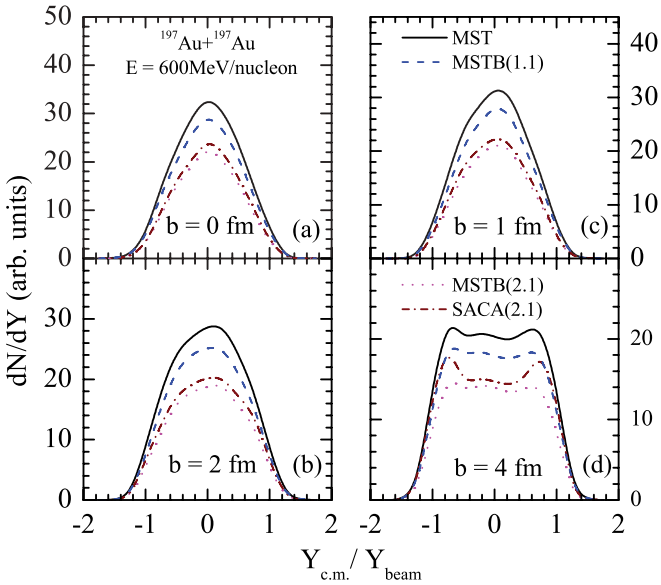

FIG. 5. (Color online) The rapidity distribution of LCPs (dN/dY) at freeze-out time (250 fm/c) for the reaction of ^{197}Au + ^{197}Au at 600 MeV/nucleon and (a) b = 0, (c) 1, (b) 2, and (d) 4 fm. The results obtained with the MST, MSTB(1.1), MSTB(2.1), and SACA(2.1) methods are shown, respectively, by solid, dashed, dotted, and dashed-dotted lines.

In Fig. 5, we display the rapidity distribution (dN/dY) of LCPs as a function of scaled rapidity ($Y/Y_{\rm beam}$) for the same reactions of ^{197}Au + ^{197}Au at b = 0–4 fm. The rapidity for the jth nucleon is defined as

$$Y(i) = \frac{1}{2} \ln \frac{\mathbf{E}(j) + \mathbf{p}_z(j)}{\mathbf{E}(j) - \mathbf{p}_z(j)}. \quad (6)$$

Here, $\mathbf{E}(j)$ and $\mathbf{p}_z(j)$ are, respectively, the total energy (nucleon) and longitudinal momentum per nucleon for the jth nucleon. Clearly, we see that a proper binding-energy cut leads to a rapidity distribution, which is closer to the most bound structure formed by SACA(2.1). We see that, in all the cases, the rapidity is much smaller compared to the MST method. We have also tested the gain factor, a quantity that measures the interaction of fragments with surroundings. This implementation is found to have far fewer interactions, indicating that fragments are realistic.

From the above analysis, it is clear that present implementation of the MST method is promising as it avoids creation and detection of spurious fragments and, in many cases, yields results close to the SACA method and to experimental data. It is worth mentioning that all methods should converge to the same result after the reaction has finished. This reaction time for such calculations is as large as 1000 fm/c [4]. At the same time, semiclassical models such as the QMD model does not keep nuclei stable for such a long time. One has tried to identify the fragments at earlier time steps. The complicated methods SACA(2.1) and ECRA depend on the set of cooling parameters, iterative procedure, identification of minima, etc., and therefore, output of clusters can vary drastically if one plays with these parameters. On the other hand, the MST method does not have any such parameter; therefore, we attempted to improve this method by employing the proper binding-energy check. Our implementation gives reasonable bound fragments, and therefore can be of help in clusterizing the phase space.

Summarizing, by using the quantum molecular dynamics model, we studied the formation and stability of the fragments formed in heavy-ion collisions. The minimum spanning tree method is improved by imposing a realistic microscopic binding-energy cut for each fragment. The results were compared with experimental data of ALADiN and also with the yields obtained with most bound calculations based on the simulated annealing technique (2.1). Our analysis reveals that the present modification improves the predictive power of the MST method in many cases.

The work was supported by a grant from the Department of Science and Technology (DST), Govt. of India.

[1] J. Aichelin, Phys. Rep. **202**, 233 (1991).
[2] M. Begemann-Blaich *et al.*, Phys. Rev. C **48**, 610 (1993); A. Schüttauf *et al.*, Nucl. Phys. A **607**, 457 (1996).
[3] M. D'Agostino *et al.*, Nucl. Phys. A **650**, 329 (1999).
[4] E. J. Garcia-Solis and A. C. Mignerey, Phys. Rev. C **54**, 276 (1996); C. O. Dorso and J. Aichelin, Phys. Lett. B **345**, 197 (1995).
[5] S. Kumar and R. K. Puri, Phys. Rev. C **58**, 2858 (1998); J. Singh and R. K. Puri, J. Phys. G: Nucl. Part. Phys. **27**, 2091 (2001).
[6] P. B. Gossiaux, R. K. Puri, C. Hartnack, and J. Aichelin, Nucl. Phys. A **619**, 379 (1997); R. K. Puri and J. Aichelin, J. Comput. Phys. **162**, 245 (2000); Y. K. Vermani, J. K. Dhawan, S. Goyal, R. K. Puri, and J. Aichelin, J. Phys. G: Nucl. Part. Phys. **37**, 015105 (2010).
[7] W. Bauer, Prog. Part. Nucl. Phys. **30**, 45 (1993).
[8] P. B. Gossiaux and J. Aichelin, Phys. Rev. C **56**, 2109 (1997).
[9] C. O. Dorso and J. Randrup, Phys. Lett. B **301**, 328 (1993).
[10] C. F. V. Weizsäcker, Z. Phys. A **96**, 431 (1935).
[11] C. Samanta and S. Adhikari, Phys. Rev. C **65**, 037301 (2002); **69**, 049804 (2004).
[12] S. Leray, C. Ngô, M. E. Spina, B. Remaud, and F. Sebille, Nucl. Phys. A **511**, 414 (1990).
[13] A. Coniglio, H. E. Stanley, and W. Klein, Phys. Rev. Lett. **42**, 518 (1979); F. Gulminelli and Ph. Chomaz, *ibid.* **82**, 1402 (1999); S. K. Samaddar and S. Das Gupta, Phys. Rev. C **61**, 034610 (2000).
[14] B. Borderie and M. F. Rivet, Prog. Part. Nucl. Phys. **61**, 551 (2008).
[15] B. Heide and H. W. Barz, Nucl. Phys. A **588**, 918 (1995).